계명의대학술지
Keimyung Medical Journal

Original Article

pISSN 2092-8335 · eISSN 2733-5380
Keimyung Med J 2022;41(2):56-66
https://doi.org/10.46308/kmj.2022.00199

Received: November 14, 2022
Revised: December 7, 2022
Accepted: December 9, 2022

Corresponding Author:
Sungwoon Choi
Department of New Drug Discovery, Chungnam National University, 99, Daehak-ro, Yuseong-gu, Daejeon 34134, Korea
E-mail: schoi@cnu.ac.kr

Byeong-Churl Jang, PhD
Department of Molecular Medicine, Keimyung University School of Medicine, 1095 Dalgubeol-daero, Dalseo-gu, Daegu 42601, Korea
Tel: +82-53-258-7404
Fax: +82-53-258-7403
E-mail: jangbc123@gw.kmu.ac.kr

*These authors equally contributed to this work.

2-Aryl Propionic Acid Amide Modification of Naproxen and Ibuprofen Dimers for Anti-neuroinflammatory Activity in BV2 mouse Microglial Cells

Hyerim Ju[1,*], Shailashree Pachhapure[2,*], Amila Mufida[2], Aryun Kim[3], David R. Elmaleh[4,5], Sungwoon Choi[1], Byeong-Churl Jang[2]

[1]Department of New Drug Discovery, Chungnam National University, Daejeon, Korea
[2]Department of Molecular Medicine, Keimyung University School of Medicine, Daegu, Korea
[3]Department of Neurology, Chungbuk National University Hospital, Cheongju, Korea
[4]AZTherapies, Inc., Boston, MA, USA
[5]Department of Radiology, Massachusetts General Hospital and Harvard Medical School, Boston, USA

Inflammation is a common link in the pathophysiology of many neurological illnesses, including Alzheimer's disease. Activated glial cells contribute to neuroinflammation by producing pro-inflammatory mediators. Naproxen and ibuprofen are nonsteroidal anti-inflammatory drugs with 2-aryl(s) propionic acid as a common pharmacophore. Here we designed a small series of naproxen and ibuprofen amide dimers and tested their effects on the expression of inducible nitric oxide synthase (iNOS), a neuroinflammatory enzyme in lipopolysaccharide (LPS)-stimulated BV2 mouse microglial cells. Of note, treatment with **CNU 019**, **020**, **021**, **023**, **024**, and **027** at 10 μM markedly inhibited the LPS-induced iNOS expression in BV2 cells. **CNU 024** was tested further at different concentrations to regulate the LPS-induced iNOS expression in BV2 cells. Treatment with **CNU 024** at 5, 10, or 20 μM dose-dependently suppressed the LPS-induced iNOS protein and mRNA expression levels in BV2 cells, in which maximal inhibition was seen at 20 μM. **CNU 024** treatment at doses tested further led to a concentration-dependent inhibition of the LPS-induced phosphorylation (activation) of p38 mitogen-activated protein kinase (MAPK) without influencing its total protein expression in BV2 cells, but it did not affect the LPS-induced activation of c-jun N-terminal kinase-1/2 and extracellular signal-regulated kinases-1/2 in these cells. In summary, our results demonstrate that **CNU 024** inhibits the LPS-induced iNOS expression in BV2 cells, partly mediated by the inhibition of p38 MAPK. This work shows that **CNU 024** could be a valuable ligand for further development as a potential drug candidate for treating neuroinflammatory pathologies.

Keywords: Lipopolysaccharide, NSAID amide dimer, Nitric Oxide Synthase Type II, p38 Mitogen-Activated Protein Kinases

Introduction

Neuroinflammation has exhibited its pivotal role in the development of many neurological illnesses, including Alzheimer's disease (AD), in response to numerous pathological conditions [1]. In central nervous system (CNS), neuroinflammation is marked as the activation of microglia, high production of pro-inflammatory cytokines, recruitment of T-cells, and neural tissue (cell) damage [2]. Accumulating evidence further indicates that various extrinsic and intrinsic stimuli, such as lipopolysaccharide (LPS), particulate matter (PM), interferon-gamma (IFN-γ), or tumor necrosis factor-alpha (TNF-α), can induce the

microglia activation, which results in the abnormal expression of many neuroinflammatory mediators, including inducible nitric oxide synthase (iNOS), TNF-α, and interleukin-1β (IL-1β), and IL-6 [3,4].

iNOS is an inflammatory enzyme responsible for the production of nitric oxide (NO) in the human body, including brain [5-7]. We and others have previously reported that LPS induces high expression of iNOS in BV2 cells, a mouse microglial cell line, and the LPS-induced iNOS expression in these cells is mediated through the activation of not only nuclear factor-kappa B (NF-κB), a transcription factor, but also multiple protein kinases, including extracellular signal-regulated kinase (ERK-1/2), p38 mitogen-activated protein kinase (MAPK), c-Jun N-terminal kinase (JNK-1/2), and protein kinase B [8-10]. Of importance, there is a large body of evidence that overexpression of iNOS (and the resultant NO overgeneration) plays a crucial role in neuroinflammation and neuronal cell death in the damaged CNS [11]. Thus, iNOS and its inhibitor are considered a key molecular target and targeted therapy against neuroinflammatory pathologies [12,13]. It is therefore conceivable that any substance that inhibits iNOS overexpression in the activated microglia or glial cells may be applied as a potential anti-neuroinflammatory agent or drug candidate molecule.

There are no specific drugs currently available to repair the damaged neurons, to induce neurodegeneration, and to prevent neuroinflammation, and current drugs are effective only for reducing the severity of symptoms by limiting the extent of neuroinflammation. A wealth of information exists that non-steroidal anti-inflammatory drugs (NSAIDs), due to their neuroprotective, anti-inflammatory, and antioxidant properties, may be used for preventing and protecting neurodegenerative illnesses [14,15], although they are associated with an increased risk of adverse gastrointestinal, renal and cardiovascular effects. It is documented that their main action mechanisms are the inactivation of cyclooxygenase-2 (COX-2), the inducible enzyme responsible for overproduction of prostaglandins and thromboxanes, known inflammation and pain inducing hormones [16,17] and the inhibition of NF-κB, the transcription factor involved in the transcriptional up-regulation of many inflammatory genes, which include iNOS, COX-2, and cytokines [18].

Emerging study is needed to develop new therapeutic agent to prevent neurological pathogenesis involving neuroinflammation or to slow its progression in the damaged CNS. It is also currently thought that neurodegenerative disorders are considered as a multifactorial disease; hence, the therapeutic strategies to combat neurological pathogenesis and/or neurodegenerative disorders should involve multiple targets instead of a single target or targeted therapy [19-21]. Naproxen and ibuprofen are known NSAIDs with neuroprotective and anti-inflammatory effects. To evaluate the structural requirement and necessity of carboxylic function in the drugs as a part of our ongoing effort to generate multi-target ligands for neurodegenerative diseases, in this study, we newly synthesized a small series of naproxen and ibuprofen amide dimers by the structural modification and tested whether these amide dimers can modulate the LPS-induced iNOS expression in BV2 cells.

Materials and methods

1. Materials

Primary antibodies for phosphorylated (p-) ERK-1/2, total (T-) ERK-1/2, p-JNK-1/2, T-JNK1/2, p-p38 MAPK, and T-p38 MAPK were purchased from Cell Signaling Tech. (Danvers, Massachusetts, USA). iNOS and IκB-α antibodies were purchased from Santa Cruz biotechnology (Dallas, Texas, USA). Enhanced chemiluminescence (ECL) reagents were purchased from Advansta (San Jose, CA, USA). The anti-actin antibody was obtained from Sigma-Aldrich (St. Louis, Mo, USA).

2. Synthesis of NSAID amide dimers

All chemicals were purchased from commercial sources and used without further purification. Silica gel 60 F-254 (0.25-mm thickness) plates were used for thin-layer chromatography (TLC) analysis and ultraviolet light and/or iodine vapor was for visualization on TLC plates. Silica gel column chromatography used for purification was performed on Merck silica gel 60 (230–400 mesh). The NMR spectra were recorded using a Burker (Fourier 300) 300 MHz or Burker (AVANCE Neo 400) 400 MHz spectrometer. All ^{1}H NMR spectra for samples are reported in δ units (ppm) and are referenced to the peak for tetramethylsilane if conducted in $CDCl_3$, or to the central line of the quintet at 2.49 ppm in d_6-DMSO. Spectral data are reported as follows: chemical shift (ppm), multiplicity (s, singlet; d, doublet; t, triplet; q, quartet; m, multiplet; br, broad), coupling constant, and integration value. Coupling constants (J) are reported in hertz.

(2S,2'S)-2,2'-(((2-Hydroxypropane-1,3-diyl)bis(oxy))bis(naphthalene-6,2-diyl))bis(N-hexylpropanamide) (**CNU 015**). A mixture of (2S,2'S)-2,2'-(((2-hydroxypropane-1,3-diyl)bis(oxy))bis(naphthalene-6,2-diyl))dipropionic acid (**1**, 70 mg, 0.143 mmol), HATU (120 mg, 0.32 mmol), n-hexylamine (31.4 mg, 0.31 mmol) and triethylamine (94 mg, 0.93 mmol) in

DMF was stirred at RT. After 16h, the mixture was poured into EtOAc, washed sequentially with diluted HCl, sat. $NaHCO_3$, brine, and dried with Na_2SO_4. Filtration, evaporation and purification of the residue by column chromatography (silica gel, 33% of EtOAc in hexane with drops of acetic acid) provided compound **CNU 015** (88.4 mg, 96.5%) as an slightly brown solid. ^{1}H-NMR (300 MHz, DMSO-d_6): δ 7.94 (br t, J = 6.0, 2 H), 7.79–7.70 (m, 6 H), 7.44–7.41 (m, 2 H), 7.33–7.32 (m, 2 H), 7.20–7.17 (m, 2 H), 5.51 (br d, J = 6.0, 1 H), 4.33–4.14 (m, 5 H), 3.70 (q, J = 7.0, 2 H), 3.01 (q, J = 6.0, 4 H), 1.39 (d, J = 9.0, 6 H, overlap with m), 1.34–1.11 (m, 16 H, overlap with d), 0.79 (t, J = 6.0, 6 H).

Di-tert-butyl 2,2'-(((2S,2'S)-2,2'-(((2-hydroxypropane-1,3-diyl)bis(oxy))bis(naphthalene-6,2-diyl))bis(propanoyl))bis(azanediyl))diacetate (**CNU 016**). Following the procedure used to prepare **CNU 015**, using (2S,2'S)-2,2'-(((2-hydroxypropane-1,3-diyl)bis(oxy))bis(naphthalene-6,2-diyl))dipropionic acid (**1**, 70 mg, 0.143 mmol), HATU (117.9 mg, 0.31 mmol), glycine 1,1-dimethylethyl ester (tert-Butyl 2-aminoacetate) (42.4 mg, 0.31 mmol) and triethylamine (94 mg, 0.93 mmol) and eluting with a 20% EtOAc in hexane provided **CNU 016** (83.6 mg, 82% yield) as an oil. ^{1}H-NMR (300 MHz, DMSO-d_6): δ 8.31 (br t, J = 6.0, 2 H), 7.80–7.73 (m, 6 H), 7.46–7.43 (m, 2 H), 7.34–7.33 (m, 2 H), 7.21–7.17 (m, 2 H), 5.49 (br, 1 H), 4.30–4.18 (m, 5 H), 3.79 (q, J = 6.0, 1 H), 3.69 (d, J = 6.0, 4 H), 1.42 (d, J = 6.0, 6 H), 1.34 (s, 18 H).

2,2'-(((2S,2'S)-2,2'-(((2-Hydroxypropane-1,3-diyl)bis(oxy))bis(naphthalene-6,2 diyl))bis(propanoyl))bis(azanediyl))diacetic acid (**CNU 017**). A suspension of compound **CNU 016** (70 mg, 0.1 mmol) in THF and 0.1 M sodium hydroxide (2.4 mL) was stirred at 0˚C for 16h. The solution was acidified with 10% HCl and volatiles were removed. The residue was extracted with EtOAc, washed with water and brine, and dried with Na_2SO_4. After filtration, evaporation and purification of the residue by column chromatography (silica gel, Hexane / EtOAc = 50%, Acetic acid 50 μL), compound **CNU 017** (46.2 mg, 78.3%) was finally obtained as a white solid. ^{1}H-NMR (300 MHz, DMSO-d_6): δ 12.55 (br, 2 H), 8.29 (br t, J = 6.0, 2 H), 7.80-7.72 (m, 6 H), 7.46-7.43 (m, 2 H), 7.34-7.33 (m, 2 H), 7.21-7.17 (m, 2 H), 5.50 (br d, J = 3.0, 1 H), 4.30-4.15 (m, 5 H), 3.81 (q, J = 7.0, 2 H, overlap with br t), 3.73 (br t, J = 6.0, 4 H, overlap with q), 1.43 (d, J = 9.0, 6 H).

2,2'-(((2-Hydroxypropane-1,3-diyl)bis(oxy))bis(4,1-phenylene))bis(N-hexylpropanamide) (**CNU 018**). Following the procedure used to prepare **CNU 015**, using 2,2'-(((2-hydroxypropane-1,3-diyl)bis(oxy))bis(4,1-phenylene))dipropionic acid (2, 80 mg, 0.2 mmol), HATU (172.24 mg, 0.45 mmol), n-hexylamine (45.85 mg, 0.45 mmol) and triethylamine (83.82 μL, 0.60 mmol) and eluting with a 20% EtOAc in hexane provided **CNU 018** (77.3 mg, 69.3% yield) as an oil. ^{1}H-NMR (300 MHz, $CDCl_3$): δ 7.24–7.20 (m, 4 H), 6.93-6.89 (m, 4 H), 5.26 (br, 2 H), 4.38 (q, J = 6.0, 1 H), 4.16-4.13 (m, 4 H), 3.49 (q, J = 7.0, 2 H). 3.17 (q, J = 6.0, 4 H), 2.56 (br d, J = 6.0, 1 H),1.50 (d, J = 9.0, 6 H), 1.41-1.19 (m, 16 H), 0.85 (t, J = 6.0, 6 H).

Di-tert-butyl 2,2'-((2,2'-(((2-hydroxypropane-1,3-diyl)bis(oxy))bis(4,1-phenylene))bis(propanoyl))bis(azanediyl))diacetate (**CNU 019**). Following the procedure used to prepare **CNU 015**, using 2,2'-(((2-hydroxypropane-1,3-diyl)bis(oxy))bis(4,1-phenylene))dipropionic acid (**2**, 100 mg, 0.26 mmol), HATU (125.21 mg, 0.57 mmol), glycine 1,1-dimethylethyl ester (tert-Butyl 2-aminoacetate) (74.30 mg, 0.57 mmol) and triethylamine (107.17 μL, 0.77 mmol) and eluting with a 20% EtOAc in hexane provided **CNU 019** (55 mg, 34.8% yield) as an oil. ^{1}H-NMR (300 MHz, DMSO-d_6): δ 7.26-7.23 (m, 4 H, overlap with s), 6.93-6.90 (m, 4 H), 5.85 (br, 2 H), 4.34 (q, J = 6.0, 1 H), 4.15-4.13 (m, 4 H), 3.96-3.75 (m, 4 H), 3.56 (q, J = 6.0, 2 H), 1.51 (d, J = 6.0, 6 H), 1.43 (s, 18 H).

2,2'-((2,2'-(((2-Hydroxypropane-1,3-diyl)bis(oxy))bis(4,1-phenylene))bis(propanoyl))bis(azanediyl))diacetic acid (**CNU 020**). Following the procedure used to prepare **CNU 017**, using **CNU 019** (120 mg, 0.2 mmol) in THF, 0.1 M sodium hydroxide (4 mL) eluting with a 20% EtOAc in hexane provided **CNU 020** (44.2 mg, 45.2% yield) as an oil. ^{1}H-NMR (300 MHz, $CDCl_3$ with DNSO-d_6): δ 7.26-7.23 (m, 4 H), 6.91-6.88 (m, 4 H), 6.61 (br, 2 H), 4.35-4.28 (m, 1 H), 4.11 (t, J = 6.0, 4 H), 4.00-3.82 (m, 4 H), 3.60 (q, J = 7.0, 2 H), 1.47 (d, J = 6.0, 6 H).

Dimethyl 2,2'-(((2S,2'S)-2,2'-(((2-hydroxypropane-1,3-diyl)bis(oxy))bis(naphthalene-6,2-diyl))bis(propanoyl))bis(azanediyl))(2R,2'R)-dipropionate (**CNU 021**). Following the procedure used to prepare **CNU 015**, using (2S,2'S)-2,2'-(((2-hydroxypropane-1,3-diyl)bis(oxy))bis(naphthalene-6,2-diyl))dipropionic acid (1, 100 mg, 0.2 mmol), HATU (228.1 mg, 0.59 mmol), D-alanine methyl ester hydrochloride (83.7 mg, 0.59 mmol) and triethylamine (83.4 μL, 0.59 mmol) and eluting with a 20% EtOAc in hexane provided **CNU 021** as a white solid (96.9 mg, 72%). ^{1}H-NMR (400 MHz, DMSO-d_6): δ 8.46-8.43 (m, 2 H), 7.80-7.71 (m, 6 H), 7.45-7.42 (m, 2 H), 7.34 (br s, 2 H), 7.21-7.18 (m, 2 H), 5.50 (br d, J = 4.0, 1 H), 4.33-4.16 (m, 7 H), 3.80 (q, J = 8.0, 2 H), 3.64 (s, 3 H), 3.52 (s, 3 H), 1.41 (d, J = 4.0, 3 H), 1.40 (d, J = 4.0, 3 H), 1.28 (d, J = 8.0, 3 H), 1.23 (d, J = 8.0, 3 H).

Dimethyl 2,2'-((2,2'-(((2-hydroxypropane-1,3-diyl)bis(oxy))bis(4,1-phenylene))bis(propanoyl))bis(azanediyl))(2R,2'R)-dipropionate (**CNU 024**). Following the procedure used to pre-

pare **CNU 015**, using 2,2'-(((2-hydroxypropane-1,3-diyl) bis(oxy))bis(4,1-phenylene))dipropionic acid (**2**, 100 mg, 0.26 mmol), HATU (293.2 mg, 0.77 mmol), D-alanine methyl ester hydrochloride (42.4 mg, 0.31 mmol) and triethylamine (107.2 μL, 0.77 mmol) and eluting with a 20% EtOAc in hexane provided **CNU 024** as a white solid (127.1 mg, 87.3%). ^{1}H-NMR (400 MHz, CDCl3): δ 7.24–7.22 (m, 4 H), 6.94-6.90 (m, 4 H), 5.93-5.88 (br m, 2 H), 4.55 (sex, J = 6.7, 2 H), 4.38 (quin, J = 6.0, 1 H), 4.15 (t, J = 6.0, 4 H), 3.72 (s, 3 H), 3.69 (s, 3 H), 3.54 (q, J = 6.7, 2 H), 2.65 (br d, J = 4.0, 1 H), 1.50–1.48 (m, 6 H), 1.34 (d, J = 8.0, 3 H), 1.29 (d, J = 8.0, 3 H).

3. Cell culture

BV2 mouse microglial cells (ATCC, Manassas, VA, USA) were grown in culture media containing Dulbecco's modified Eagle's medium (DMEM) (Welgene, Daegu, Korea) supplemented with 10% heat-inactivated fetal bovine serum (FBS) (Gibco, Grand Island, NY, USA) and 1% penicillin/streptomycin (Welgene) at 37°C in a humidified atmosphere of 5% CO_2.

4. Preparation of whole-cell lysates

After material treatments with the designated concentrations or time point, BV2 cells were washed with PBS and lysed in a modified radio-immunoprecipitated assay buffer (50 mM Tris-Cl [pH 7.4], 150 mM NaCl, 0.1% sodium dodecyl sulfate, 0.25% sodium deoxycholate, 1% Triton X-100, 1% Nonidet P-40, 1 mM EDTA, 1 mM EGTA, proteinase inhibitor cocktail [1x]). The whole-cell lysates were collected and centrifuged at 14,000 rpm for 15 min at 4°C. The supernatant was preserved, and its protein concentration was determined with Pierce BCA Protein Assay Kit (Thermo Scientific, Rockford, IL, USA).

5. Western blot analysis

An aliquot of proteins (50 μg) were separated by 10% sodium dodecyl sulfate-polyacrylamide (SDS-PAGE) and transferred onto nitrocellulose membranes (Millipore Co., Bedford, MA, USA). The membranes were washed with Tris-buffered saline (TBS) (10 mM Tris, 150 mM NaCl) supplemented with 0.05% (v/v) Tween-20 (TBST) and blocked with the blocking buffer (TBST containing 5% (w/v) non-fat dried milk). The membranes were incubated overnight with respective primary antibody of p-ERK-1/2 (1:2,000), T-ERK-1/2 (1:2,000), p-JNK-1/2 (1:2,000), T-JNK-1/2 (1:2,000), p-p38 MAPK (1:2,000), T-p38 MAPK (1:2,000), IκB-α (1:2,000), iNOS (1:1,000), or actin (1:10,000) at 4°C. The membranes were washed with TBST and then incubated with secondary antibodies coupled to horseradish peroxidase for 2 h. The membranes were then washed with TBST. Enzyme-linked chemiluminescence (ECL) reagents (Advansta, San Jose, CA, USA) was used to develop the image. Equal loading of proteins was verified by actin antibody.

6. Reverse transcription-polymerase chain reaction (RT-PCR) analysis

After material treatments with the designated concentrations or time point, total RNA from the conditioned BV2 cells was extracted using RNAiso Plus (TaKaRa, Kusatsu, Shiga, Japan). Random hexadeoxynucleotide primer and reverse transcriptase were used for reverse transcribed the total RNA (3 μg). The single-strand cDNA was then amplified by PCR with specific sense and antisense primer of iNOS or actin. The primer sequences used for PCR were as follows: iNOS forward 5'GACAAGCTGCATGTAACATC, and reverse GCTGGTAGGTTCCTGTTGTT3'; actin forward 5'-GGT GAA GGT CGG TGT GAA CG-3'; reverse 5'-GGT AGG AAC ACG GAA GGC CA-3'. Expression levels of actin mRNA were used to evaluate the relative mRNA expression of iNOS.

Results

1. Dimer amide design and synthesis

Our synthetic effort to mask carboxylic acid with biologically labile amide bond generated eight new compounds (Fig. 1A-C) in low to moderate yields. For the introduction of amide function, the amino part of protected glycine (**CNU 016**, **017**, **019**, and **020**) or alanine methyl ester (**CNU 021** and **024**) were conjugated. In addition, in order to evaluate the structural requirement for the biological activity the carboxylic part of new amide dimers were exposed (**CNU 017** and **020**). The conjugated derivatives with amines at the position of aryl propionic acid of NSAIDs were reported, but the amide dimers (**4**, Fig. 1A) were never investigated for the neuroinflammation modulation. The ibuprofen-type and naproxen-type amide dimers were synthesized from carboxylic acid (**2**, **3**, Fig. 1A and 1C) with amine or two equivalents of methyl or t-butyl esters of amide monomer having aryl phenol were reacted with epichlorohydrin under K_2CO_3 basic conditions to give amide dimers in moderate yield (no experimental and characterization details for **CNU 022**, **023**, **025-027** were provided for the reason of patent and will be reported later).

2. Effects of synthesized amide dimers on the LPS-induced iNOS expression in BV2 cells

We next investigated the effect of synthesized amide dimers

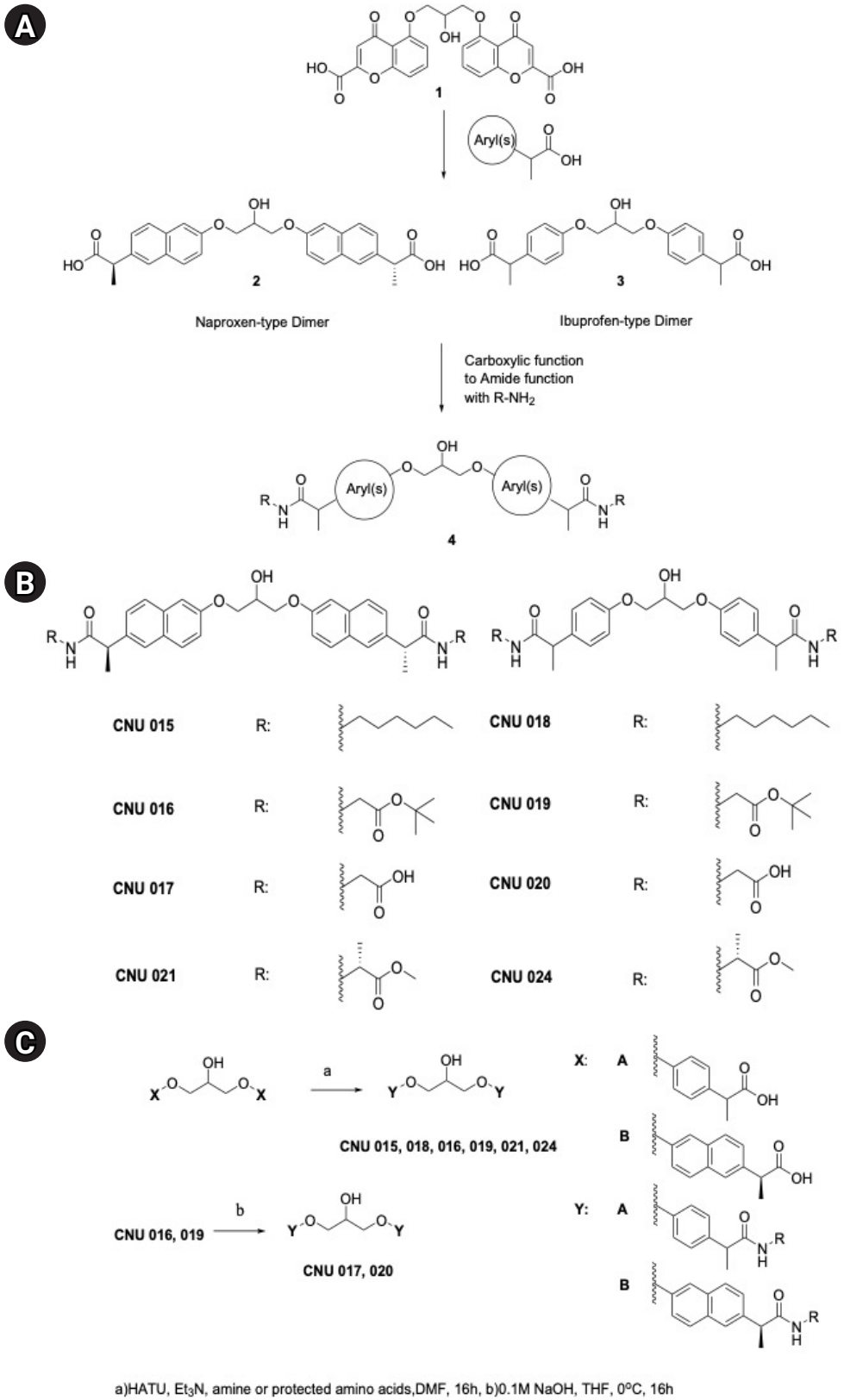

Fig. 1. Design and structures of aryl propionic acid amide dimers. (A) Design flow for the preparation of NSAID amide dimers from cromoglicic acid (1). (B) Chemical structures of prepared NSAID amide dimers. (C) Schematic synthetic flow for the NSAID amide dimers.

at a concentration of 10 μM on the LPS-induced iNOS expression in BV2 cells for 8 h by using Western blot analysis. As shown in Fig. 2A-C, compared with control (no LPS), there was an elevated iNOS expression in BV2 cells only when exposed to LPS for 8 h. Of note, BV2 cells treated with **CNU 019**, **CNU 020**, **CNU 021**, **CNU 023**, **CNU 024**, and **CNU 027**, respectively, exhibited a substantial reduction in iNOS protein expression levels compared with control. On the contrary, there was no effect on the LPS-induced iNOS expression BV2 cells treated with **CNU 025** or **026** compared with control; rather they slightly enhanced it. Total protein expression levels of actin, used and included as an internal control herein, remained constant under these experimental conditions. Due to the strong inhibitory effect on the LPS-induced iNOS expression in BV2 cells, we selected **CNU 024** for further studies (No experimental details and results for **CNU 015**-**017** were provided for the reason of different cell lines used and negative results).

3. CNU 024 at 20 μM has a strong inhibitory effect on the LPS-induced iNOS expression in BV2 cells

We next tested the effect of **CNU 024** at different concentrations (5, 10, or 20 μM) on the LPS-induced iNOS protein expression in BV2 cells for 8 h. As shown in Fig. 3A, treatment with **CNU 024** resulted in a concentration-dependent inhibition of the LPS-induced iNOS expression in BV2 cells in which maximal inhibition was seen at 20 μM. Total protein expression levels of actin remained unchanged under these experimental conditions. To see whether the **CNU 024**'s inhibition of the LPS-induced iNOS protein expression herein was due to iNOS transcriptional down-regulation, we next measured the effect of **CNU 024** at 5, 10, or 20 μM on the LPS-induced iNOS expression at the mRNA levels in BV2 cells for 8 h by using RT-PCR analysis. As shown in Fig. 3B, treatment with control (no LPS), LPS induced an elevation of iNOS transcripts in BV2 cells. Distinctly, while **CNU 024** treatment at 5 or 10 μM had no inhibitory effect on the LPS-induced iNOS mRNA expression in BV2 cells, treatment with **CNU 024** at 20

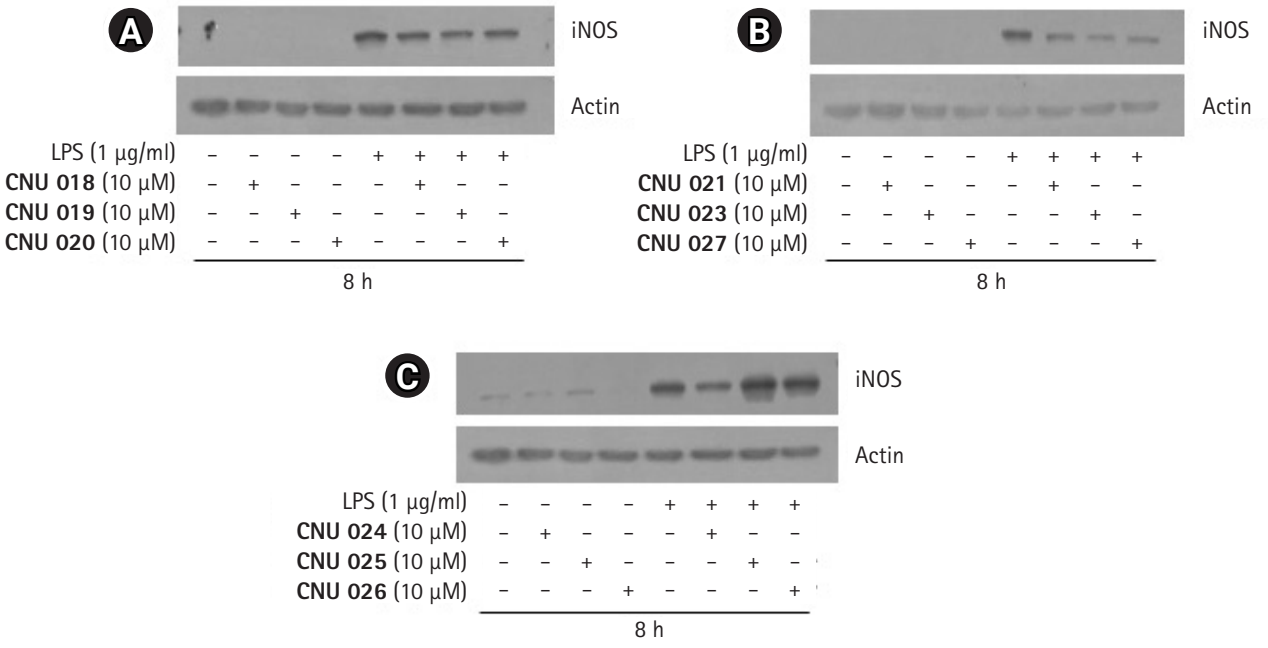

Fig. 2. Effect of 9 aryl propionic acid amide derivatives on expression of iNOS at the protein levels in LPS-stimulated BV2 mouse microglial cells. (A) BV2 cells were treated without or with LPS (1 μg/mL) in the absence or presence of **CNU 018**, **019**, or **020** at 10 μM concentration for 8 h. Whole-cell lysates were prepared and analyzed by Western blotting. (B) BV2 cells were treated without or with LPS (1 μg/mL) in the absence or presence of **CNU 021**, **023**, or **027** at 10 μM concentration for 8 h. Whole-cell lysates from the conditioned cells were prepared and analyzed by Western blotting. (C) BV2 cells were treated without or with LPS (1 μg/mL) in the absence or presence of **CNU 024**, **025**, or **026** at 10 μM concentration for 8 h. Whole-cell lysates from the conditioned cells were prepared and analyzed by Western blotting.

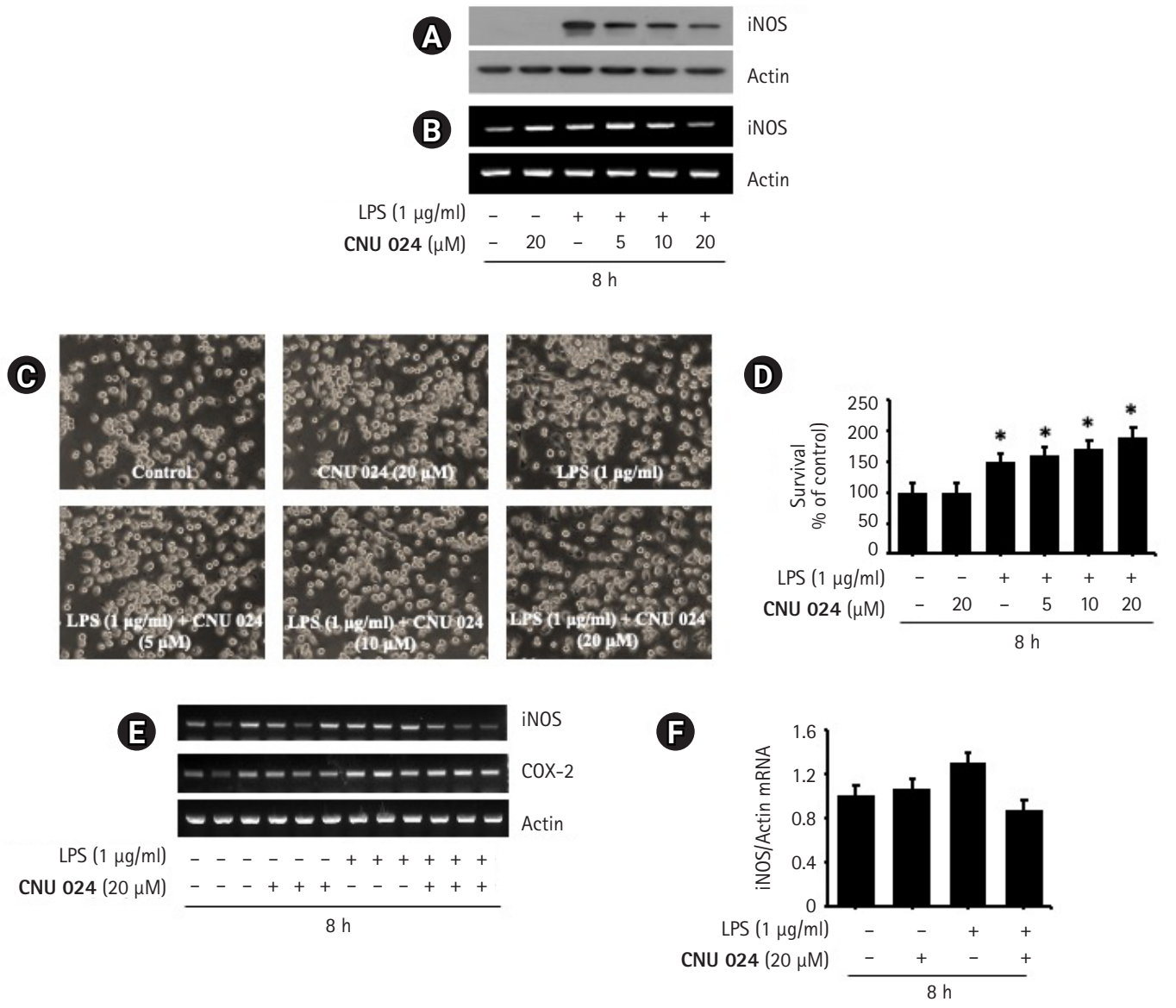

Fig. 3. Effect of **CNU 024** at different concentrations on expression of iNOS at the protein and mRNA levels in BV2 mouse microglial cells. (A) BV2 cells were treated without or with LPS (1 μg/mL) in the absence or presence of **CNU 024** at different concentrations (5, 10, or 20 μM) for 8 h. Whole-cell lysates from the conditioned cells were prepared and analyzed by Western blotting. (B) BV2 cells were treated without or with LPS (1 μg/mL) in the absence or presence of **CNU 024** at different concentrations (5, 10, or 20 μM) for 8 h. Total RNA from the conditioned cells was prepared and analyzed by RT-PCR. (C) Phase-contrast images of BV2 cells in the presence or absence of **CNU 024** and or LPS at the indicated concentrations. (D) Measurement of the number of live cells in control or LPS-induced iNOS expression with or without **CNU 024** treatment in different concentrations by cell count assay. Data are mean ± SE from three independent experiments, each done in triplicate. *$p < 0.05$ vs. control. (E) RT-PCR analysis in triplicate experiments. (F) The densitometry result of (E) for the expression levels of iNOS normalized to those of control actin.

μM markedly repressed the agonist-induced iNOS mRNA expression in these cells. Total mRNA expression levels of actin remained constant under these experimental conditions. These results collectively demonstrate the ability of **CNU 024** at 20 μM to strongly inhibit the LPS-induced iNOS expression in BV2 cells. The effect of **CNU 024** on microglial cells morphology was assessed next. Primary cultured microglia were exposed to 1 μg/mL LPS in the absence or presence of **CNU 024** in different concentrations. As expected, most cells treated with vehicle had a ramified shape, which is the typical mor-

phology of resting microglia (Fig. 3C). In addition, the morphology of cells treated with or without **CNU 024** and LPS also did not show any difference in shape of the microglia. Of note, as shown in Fig. 3D, **CNU 024** increased these cells' survival by approximately 80% in a dose-dependent manner. Triplicate experiments confirmed the ability of **CNU 024** at 20 μM to significantly reduce the mRNA expression levels of iNOS, but not COX-2 in BV2 cells treated by LPS (Fig. 3E). The densitometry results of Fig. 3E for iNOS expression levels standardized to those of control actin is shown in Fig. 3F.

4. CNU 024 at 20 μM exhibits a strong suppressive effect on the LPS-induced p38 MAPK phosphorylation in BV2 cells

We next probed whether **CNU 024** modulates the LPS-induced activation of three members of the MAPK family (ERK-1/2, p38 MAPK, and JNK-1/2) and NF-κB, which are reported to be crucial for the agonist-induced iNOS expression in BV2 cells [22,23]. In this study, the activation or inhibition of NF-κB in BV2 cells in response to LPS and/or **CNU 024** was assessed by measuring expression levels of IκB-α, an inhibitory cytosolic protein of NF-κB [24,25]. As shown in Fig. 4A, compared with control (no LPS), treatment with LPS at 1 μg/ml for 0.5 h led to a strong phosphorylation of ERK-1/2, p38 MAPK, and JNK-1/2 without influencing respective total protein expression in BV2 cells, pointing out the LPS-induced activation of these MAPKs. As shown in Fig. 4B, the same treatment with LPS also caused a complete loss of IκB-α in BV2 cells compared with control, supporting the agonist-induced activation of NF-κB. Distinctly, while treatment with **CNU 024** at doses tested did not largely affect the LPS-induced phosphorylation of ERK-1/2 and JNK-1/2 in BV2 cells, it resulted in a dose-dependent inhibition of the LPS-induced phosphorylation of p38 MAPK in these cells. Total expression levels of ERK-1/2, p38 MAPK, and JNK-1/2 remained unchanged under these experimental conditions. **CNU 024** treatment at 20 μM also had no effect on the LPS-induced loss of IκB-α in BV2 cells. These results collectively demonstrate the ability of **CNU 024** at 20 μM to strongly and selectively inhibit the LPS-induced p38 MAPK activation in BV2 cells.

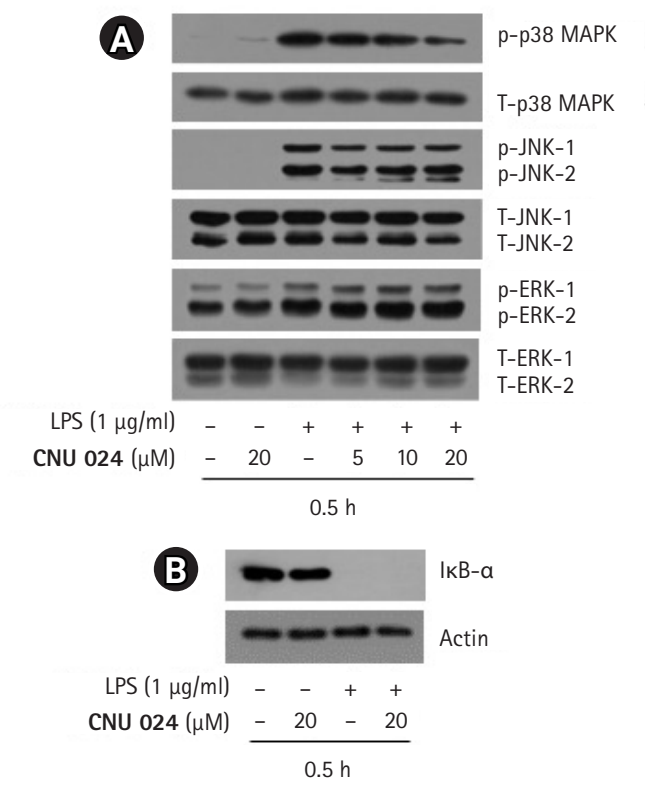

Fig. 4. Effect of **CNU 024** at different concentrations on phosphorylation and expression levels of ERK-1/2, JNK-1/2, p38 MAPK, and IκB-α in LPS-stimulated BV2 mouse microglial cells. (A) BV2 cells were treated without or with LPS (1 μg/mL) in the absence or presence of **CNU 024** at different concentrations (5, 10, or 20 μM) for 0.5 h. Whole-cell lysates from the conditioned cells were prepared and analyzed by Western blotting. p-ERK-1/2, phosphorylated ERK-1/2; T-ERK-1/2, total ERK-1/2; p-JNK-1/2, phosphorylated JKN-1/2; T-JNK-1/2, total JNK-1/2; p38 MAPK, phosphorylated p38 MAPK; T-p38 MAPK, total p38 MAPK. (B) BV2 cells were treated without or with LPS (1 μg/mL) in the absence or presence of **CNU 024** at 20 μM for 0.5 h. Whole-cell lysates from the conditioned cells were prepared and analyzed by Western blotting.

Discussion

Microglia activation results in an abnormal elevation of many inflammatory mediators including iNOS and it has been linked to the pathogenesis of neuroinflammation-related neurological disorders. The present study is designed to test a small series of naproxen and ibuprofen amide dimers and evaluate whether these amide dimers have anti-neuroinflammatory effects on the LPS-induced iNOS expression in BV2 mouse microglial cells, a well-established in vitro model of neuroinflammation. Here we show that **CNU 024**, one of NSAID amide dimers, strongly inhibits the LPS-induced iNOS expression at the protein and mRNA levels in BV2 cells. Our data further provide that the **CNU 024**'s inhibitory effect on the LPS-induced iNOS expression in BV2 cells is partly due to the inactivation of p38 MAPK pathway.

It has been reported that the disodium salt of cromoglicic acid (**1**, Fig. 1A) used mainly for asthma [26] has the anti-Aβ

aggregation property in vitro and reduces the AD-associated Aβ protein expression levels by increasing microglial phagocytosis [27,28]. NSAIDs, such as ibuprofen and naproxen, that are used to treat pain, fever, and inflammation, are shown to possess anti-aggregation properties of Aβ proteins and anti-neuroinflammatory activities [29-32]. Notably, our previous studies have shown that the replacement of chromone rings in cromoglicic acid (**1**, Fig. 1A) with 2-aryl propionic acids as a part of pharmacophore in NSAIDs provides dimer structure (**2**, naproxen-type and **3**, ibuprofen-type dimers, Fig. 1A) with anti-neuroinflammatory function and Aβ aggregation inhibition (data not shown). However, the presence of carboxylic acid moiety still can cause the gastrointestinal side effects as shown by NSAIDs having 2-aryl(s) propionic acid moiety and low brain uptake [33,34]. One of the approaches to address this problem could be masking carboxylic function with appropriate molecules as in a form of amide linkage while maintaining anti-neuroinflammatory function (**4**, Fig. 1A). Pharmacokinetic studies of naproxen amides have pointed out some amino acid esters with promising colorectal cancer chemopreventive activity [35]. Therefore, in this study, we investigated whether the structural modification with amide function of two NSAIDs naproxen and ibuprofen still hold the ability to modulate neuroinflammation, and to evaluate the necessity of carboxylic function as a part of our ongoing effort to generate multi-target ligands for AD [36].

In accordance with this understanding, we screened 8 compounds derived from 2-aryl propionic acid amide modification of naproxen and ibuprofen dimers and conveyed that among them, **CNU 019**, **020**, **021**, **023**, **024**, and **027** at 10 μM for 8 h, showed anti-inflammatory effect by substantially inhibiting iNOS expression induced by LPS in BV2 cells (Fig. 2A-C). Through additional dose-response experiments, we further confirmed the ability of **CNU 024** mainly at 20 μM to vastly inhibit the LPS-induced iNOS expression at the protein and mRNA levels in BV2 cells (Fig. 3A, B). These results strongly point out that **CNU 024** exerts its inhibitory effect on the LPS-induced iNOS expression through the iNOS transcriptional downregulation in BV2 cells.

It is known that neuroinflammation is increased in the damaged brain, which could be found in many neurological disorders, and it can be induced by the activation of NF-κB [24,25]. NF-κB is a family of structurally related transcription factors that is involved in the control of various inflammatory and immune responses, cell growth and apoptosis [37]. Several inducers including LPS have been known as NF-κB activator [37]. Accordingly, the LPS-induced NF-κB activation is mainly mediated though rapid proteolysis (protein degradation) of IκB-α, the NF-κB inhibitory cytosolic protein [24], which is crucial for the agonist-induced iNOS expression in BV2 cells [38]. In agreement with it, here, we demonstrated the activation of NF-κB in BV2 cells exposed to LPS for 0.5 h, as evidenced by the agonist's ability to completely deplete the expression levels of IκB-α (Fig. 4B). Up to date, **CNU 024**'s regulation of the LPS-induced NF-κB activation (proteolysis of IκB-α) in BV2 cells is not reported. The present study, however, showed that the LPS-induced proteolysis of IκB-α in BV2 cells is not influence by **CNU 024**. Reportedly, the LPS-induced iNOS expression in BV2 cells are associated with not only NF-κB but also other transcriptional factors [22]. It is thus likely that the **CNU 024**'s inhibitory effect on the LPS-induced iNOS expression in BV2 cells is mediated not through regulation of NF-κB/IκB-α but via that of other transcriptional factors and signaling pathways or components.

Studies have previously shown that activation of the MAPK family, including ERK-1/2, JNK-1/2, and p38 MAPK, are important for the LPS-induced iNOS expression in BV2 cells, [39,40]. In the current study, treatment with LPS for 0.5 h leads to the phosphorylation (activation) of p38 MAPK, ERK-1/2, and JNK-1/2 in BV2 cells (Fig. 4A), supporting the LPS's stimulating effects on these signaling components. Of note, we observed that **CNU 024** at 20 μM dramatically lowers the LPS-induced phosphorylated levels of p38 MAPK in BV2 cells, whereas it does not influence the agonist-induced phosphorylated levels of ERK-1/2 and JNK-1/2 in these cells. These results strongly indicate that **CNU 024** exerts its inhibitory effect on the LPS-induced iNOS expression in BV2 cells not through regulation of the ERK-1/2 and JNK-1/2 but via control (inhibition) of the p38 MAPK and its downstream signaling pathway.

Conclusions

It is the first study to demonstrate that **CNU 024**, one of the NSAID amide dimers, strongly suppresses the induction of iNOS expression in LPS-stimulated BV2 murine microglial cells, and the suppression is partly due to the selective inhibition of p38 MAPK. This work shows that **CNU 024** could be a valuable ligand for further development as a potential drug candidate for treating neuroinflammatory pathologies.

Conflict of interest

The authors declare no conflicts-of-interest related to this article.

References

1. Leng F, Edison P. Neuroinflammation and microglial activation in Alzheimer disease: where do we go from here? Nat Rev Neurol. 2021;17:157-72.
2. Estes ML, McAllister AK. Alterations in immune cells and mediators in the brain: it's not always neuroinflammation! Brain Pathol. 2014;24:623-30.
3. Esshili A, Manitz MP, Freund N, Juckel G. Induction of inducible nitric oxide synthase expression in activated microglia and astrocytes following pre- and postnatal immune challenge in an animal model of schizophrenia. Eur Neuropsychopharmacol. 2020;35:100-10.
4. Wang WY, Tan MS, Yu JT, Tan L. Role of pro-inflammatory cytokines released from microglia in Alzheimer's disease. Ann Transl Med. 2015;3:136.
5. Sierra A, Navascués J, Cuadros MA, Calvente R, Martín-Oliva D, Ferrer-Martín RM, et al. Expression of inducible nitric oxide synthase (iNOS) in microglia of the developing quail retina. PLoS One. 2014;9:e106048.
6. Melih D. Role of Nitric Oxide Synthase in Normal Brain Function and Pathophysiology of Neural Diseases. In: Saravi SSS, editor. Nitric Oxide Synthase. Rijeka: IntechOpen; 2017. Available from: https://doi.org/10.5772/67267.
7. Sonar SA, Lal G. The iNOS activity during an immune response controls the CNS pathology in experimental autoimmune encephalomyelitis. Front Immunol. 2019;10:710.
8. Kim AR, Lee MS, Choi JW, Utsuki T, Kim JI, Jang BC, et al. Phlorofucofuroeckol A suppresses expression of inducible nitric oxide synthase, cyclooxygenase-2, and pro-inflammatory cytokines via inhibition of nuclear factor-κB, c-Jun NH2-terminal kinases, and Akt in microglial cells. Inflammation. 2013;36:259-71.
9. Bae JH, Jang BC, Suh SI, Ha E, Baik HH, Kim SS, et al. Manganese induces inducible nitric oxide synthase (iNOS) expression via activation of both MAP kinase and PI3K/Akt pathways in BV2 microglial cells. Neurosci Lett. 2006;398:151-4.
10. Choi Y, Lee MK, Lim SY, Sung SH, Kim YC. Inhibition of inducible NO synthase, cyclooxygenase-2 and interleukin-1beta by torilin is mediated by mitogen-activated protein kinases in microglial BV2 cells. Br J Pharmacol. 2009;156:933-40.
11. Liy PM, Puzi NNA, Jose S, Vidyadaran S. Nitric oxide modulation in neuroinflammation and the role of mesenchymal stem cells. Exp Biol Med (Maywood). 2021;246:2399-406.
12. Justo AFO, Suemoto CK. The modulation of neuroinflammation by inducible nitric oxide synthase. J Cell Commun Signal. 2022;16:155-8.
13. Qu W, Cheng Y, Peng W, Wu Y, Rui T, Luo C, et al. Targeting iNOS alleviates early brain injury after experimental subarachnoid hemorrhage via promoting ferroptosis of M1 microglia and reducing neuroinflammation. Mol Neurobiol. 2022;59:3124-39.
14. Lleo A, Galea E, Sastre M. Molecular targets of non-steroidal anti-inflammatory drugs in neurodegenerative diseases. Cell Mol Life Sci. 2007;64:1403-18.
15. Klegeris A, McGeer PL. Non-steroidal anti-inflammatory drugs (NSAIDs) and other anti-inflammatory agents in the treatment of neurodegenerative disease. Curr Alzheimer Res. 2005;2:355-65.
16. Ricciotti E, FitzGerald GA. Prostaglandins and inflammation. Arterioscler Thromb Vasc Biol. 2011;31:986-1000.
17. Jang Y, Kim M, Hwang SW. Molecular mechanisms underlying the actions of arachidonic acid-derived prostaglandins on peripheral nociception. J Neuroinflammation. 2020;17:30.
18. Kempuraj D, Thangavel R, Natteru PA, Selvakumar GP, Saeed D, Zahoor H, et al. Neuroinflammation Induces Neurodegeneration. J Neurol Neurosurg Spine. 2016;1.
19. Ozben T, Ozben S. Neuro-inflammation and anti-inflammatory treatment options for Alzheimer's disease. Clin Biochem. 2019;72:87-9.
20. Ajmone-Cat MA, Bernardo A, Greco A, Minghetti L. Non-steroidal anti-inflammatory drugs and brain inflammation: effects on microglial functions. Pharmaceuticals (Basel). 2010;3:1949-65.
21. Krause DL, Müller N. Neuroinflammation, microglia and implications for anti-inflammatory treatment in Alzheimer's disease. Int J Alzheimers Dis. 2010;2010. DOI: 10.4061/2010/732806.
22. Cai Y, Cho GS, Ju C, Wang SL, Ryu JH, Shin CY, et al. Activated microglia are less vulnerable to hemin toxicity due to nitric oxide-dependent inhibition of JNK and p38 MAPK activation. J Immunol. 2011;187:1314-21.
23. Bhatia HS, Roelofs N, Muñoz E, Fiebich BL. Alleviation of microglial activation induced by p38 MAPK/MK2/PGE(2) axis by capsaicin: potential involvement of other than TRPV1 mechanism/s. Sci Rep. 2017;7:116.
24. Oeckinghaus A, Ghosh S. The NF-kappaB family of transcription factors and its regulation. Cold Spring Harb Perspect Biol. 2009;1:a000034.
25. Christian F, Smith EL, Carmody RJ. The regulation of NF-κB subunits by phosphorylation. Cells. 2016;5.
26. Cairns H, Fitzmaurice C, Hunter D, Johnson PB, King J, Lee TB, et al. Synthesis and structure-activity relationships of disodium cromoglycate and some related compounds. J Med Chem. 1972;15:583-9.
27. Hori Y, Takeda S, Cho H, Wegmann S, Shoup TM, Takahashi K,

et al. A food and drug administration-approved asthma therapeutic agent impacts amyloid β in the brain in a transgenic model of Alzheimer disease. J Biol Chem. 2015;290:1966-78.
28. Zhang C, Griciuc A, Hudry E, Wan Y, Quinti L, Ward J, et al. Cromolyn reduces levels of the Alzheimer's disease-associated amyloid β-protein by promoting microglial phagocytosis. Sci Rep. 2018;8:1144.
29. Azam F, Alabdullah NH, Ehmedat HM, Abulifa AR, Taban I, Upadhyayula S. NSAIDs as potential treatment option for preventing amyloid β toxicity in Alzheimer's disease: an investigation by docking, molecular dynamics, and DFT studies. J Biomol Struct Dyn. 2018;36:2099–117.
30. Thomas T, Nadackal TG, Thomas K. Aspirin and non-steroidal anti-inflammatory drugs inhibit amyloid-beta aggregation. Neuroreport. 2001;12:3263-7.
31. Kim S, Chang WE, Kumar R, Klimov DK. Naproxen interferes with the assembly of Aβ oligomers implicated in Alzheimer's disease. Biophys J. 2011;100:2024-32.
32. Gasparini L, Ongini E, Wenk G. Non-steroidal anti-inflammatory drugs (NSAIDs) in Alzheimer's disease: old and new mechanisms of action. J Neurochem. 2004;91:521-36.
33. Halen PK, Murumkar PR, Giridhar R, Yadav MR. Prodrug designing of NSAIDs. Mini Rev Med Chem. 2009;9:124-39.
34. Husain A. Amide derivatives of sulfonamides and isoniazid: synthesis and biological evaluation. Acta Pol Pharm. 2009;66:513-21.
35. Aboul-Fadl T, Al-Hamad SS, Fouad EA. Pharmacokinetic studies of naproxen amides of some amino acid esters with promising colorectal cancer chemopreventive activity. Bioorg Chem. 2018;76:370-9.
36. Benek O, Korabecny J, Soukup O. A perspective on multi-target drugs for Alzheimer's disease. Trends Pharmacol Sci. 2020;41:434-45.
37. Ju Hwang C, Choi DY, Park MH, Hong JT. NF-κB as a key mediator of brain inflammation in Alzheimer's disease. CNS Neurol Disord Drug Targets. 2019;18:3-10.
38. Aid S, Langenbach R, Bosetti F. Neuroinflammatory response to lipopolysaccharide is exacerbated in mice genetically deficient in cyclooxygenase-2. J Neuroinflammation. 2008;5:17.
39. Lee JW, Bae CJ, Choi YJ, Kim SI, Kim NH, Lee HJ, et al. 3,4,5-trihydroxycinnamic acid inhibits LPS-induced iNOS expression by suppressing NF-κB activation in BV2 microglial cells. Korean J Physiol Pharmacol. 2012;16:107-12.
40. Jang BC, Paik JH, Kim SP, Shin DH, Song DK, Park JG, et al. Catalase induced expression of inflammatory mediators via activation of NF-kappaB, PI3K/AKT, p70S6K, and JNKs in BV2 microglia. Cell Signal. 2005;17:625-33.